

RESEARCH ARTICLE

The novel reversible LSD1 inhibitor SP-2577 promotes anti-tumor immunity in SWItch/Sucrose-NonFermentable (SWI/SNF) complex mutated ovarian cancer

Raffaella Soldi¹, Tithi Ghosh Halder¹, Alexis Weston¹, Trason Thode¹, Kevin Drenner¹, Rhonda Lewis¹, Mohan R. Kaadige¹, Shreyesi Srivastava², Sherin Daniel Ampanattu¹, Ryan Rodriguez del Villar¹, Jessica Lang³, Hariprasad Vankayalapati⁴, Bernard Weissman⁵, Jeffrey M. Trent³, William P. D. Hendricks³, Sunil Sharma^{1*}

1 Applied Cancer Research and Drug Discovery Division, Translational Genomics Research Institute (TGen) of City of Hope, Phoenix, Arizona, United States of America, **2** HonorHealth Clinical Research Institute, Scottsdale, Arizona, United States of America, **3** Integrated Cancer Genomics Division, Translational Genomics Research Institute (TGen) of City of Hope, Phoenix, Arizona, United States of America, **4** Huntsman Cancer Institute, University of Utah, Salt Lake City, Utah, United States of America, **5** Department of Pathology and Laboratory Medicine, Lineberger Cancer Center, University of North Carolina, Chapel Hill, North Carolina, United States of America

* ssharma@tgen.org



OPEN ACCESS

Citation: Soldi R, Ghosh Halder T, Weston A, Thode T, Drenner K, Lewis R, et al. (2020) The novel reversible LSD1 inhibitor SP-2577 promotes anti-tumor immunity in SWItch/Sucrose-NonFermentable (SWI/SNF) complex mutated ovarian cancer. *PLoS ONE* 15(7): e0235705. <https://doi.org/10.1371/journal.pone.0235705>

Editor: Srinivas Saladi, Massachusetts Eye and Ear Infirmary, Harvard Medical School, UNITED STATES

Received: February 18, 2020

Accepted: June 20, 2020

Published: July 10, 2020

Copyright: © 2020 Soldi et al. This is an open access article distributed under the terms of the [Creative Commons Attribution License](https://creativecommons.org/licenses/by/4.0/), which permits unrestricted use, distribution, and reproduction in any medium, provided the original author and source are credited.

Data Availability Statement: All relevant data are within the manuscript and its Supporting Information files.

Funding: The author(s) received no specific funding for this work.

Competing interests: Dr. Sunil Sharma declares ownership of stocks from Salaris Pharmaceuticals and he is an inventor on the patent for SP-2577 compound. Dr. Soldi declares

Abstract

Mutations of the SWI/SNF chromatin remodeling complex occur in 20% of all human cancers, including ovarian cancer. Approximately half of ovarian clear cell carcinomas (OCCC) carry mutations in the SWI/SNF subunit ARID1A, while small cell carcinoma of the ovary hypercalcemic type (SCCOHT) presents with inactivating mutations of the SWI/SNF ATPase SMARCA4 alongside epigenetic silencing of the ATPase SMARCA2. Loss of these ATPases disrupts SWI/SNF chromatin remodeling activity and may also interfere with the function of other histone-modifying enzymes that associate with or are dependent on SWI/SNF activity. One such enzyme is lysine-specific histone demethylase 1 (LSD1/KDM1A), which regulates the chromatin landscape and gene expression by demethylating proteins such as histone H3. Cross-cancer analysis of the TCGA database shows that LSD1 is highly expressed in SWI/SNF-mutated tumors. SCCOHT and OCCC cell lines have shown sensitivity to the reversible LSD1 inhibitor SP-2577 (Seclidemstat), suggesting that SWI/SNF-deficient ovarian cancers are dependent on LSD1 activity. Moreover, it has been shown that inhibition of LSD1 stimulates interferon (IFN)-dependent anti-tumor immunity through induction of endogenous retroviral elements and may thereby overcome resistance to checkpoint blockade. In this study, we investigated the ability of SP-2577 to promote anti-tumor immunity and T-cell infiltration in SCCOHT and OCCC cell lines. We found that SP-2577 stimulated IFN-dependent anti-tumor immunity in SCCOHT and promoted the expression of PD-L1 in both SCCOHT and OCCC. Together, these findings suggest that the combination therapy of SP-2577 with checkpoint inhibitors may induce or augment immunogenic responses of SWI/SNF-mutated ovarian cancers and warrants further investigation.

ownership of stocks from Salaris Pharmaceuticals. This does not alter our adherence to PLOS ONE policies on sharing data and materials. The other authors have declared that no other competing interests exist.

Introduction

An increasing number of cancers are recognized to be driven partly by inactivation of subunits in the SWI/SNF complex, a multi-protein ATP-dependent chromatin-remodeling complex with central roles in cell differentiation programs [1, 2]. Pathogenic SWI/SNF mutations occur across diverse adult cancers, typically in a genomic background of numerous other driver mutations and/or genomic instability [3, 4]. However, SWI/SNF driver mutations also occur in a unique subset of more uniform cancers, such as small cell carcinoma of the ovary hypercalcemic type (SCCOHT) [5], rhabdoid tumors (RT) [6, 7], thoracic sarcomas [8, 9], and renal medullary cancers [10]. These cancers share genetic and phenotypic features even though they arise from different anatomic sites [1]. Shared features include poorly differentiated morphology, occurrence in young populations, and clinically aggressive behavior [11, 12]. Their genetic makeup is relatively simple, with an overall low tumor mutation burden, few structural defects, and, in most cases, universal inactivation of a single subunit in the SWI/SNF complex. Particularly in ovarian cancers (OCs), the most lethal gynecologic malignancies in the developed world and the fifth leading cause of cancer-associated mortality among women in the United States [13], SWI/SNF alterations vary in different histologic subtypes. The ARID1A (BAF250a) subunit is mutated in approximately 50% of ovarian clear cell carcinomas (OCCC) and 30% of ovarian endometrioid carcinomas (OEC) [14]. SCCOHT [15], a rare and very aggressive OC, is a single-gene disease with inactivating mutations in the subunit SMARCA4 (BRG1) [16–18] and epigenetic silencing of SMARCA2 (BRM) expression [17]. SCCOHT is the most common undifferentiated ovarian malignant tumor in women under 40 years. In contrast, OCCC targets women aged 55 years or older and is characterized by mutations in phosphatidylinositol-4, 5-bisphosphate 3-kinase catalytic subunit α (PIK3CA) [19, 20], and phosphatase and tensin homolog (PTEN), in addition to the ARID1A mutations. Both SCCOHT and OCCC respond poorly to conventional chemotherapy, and to date, there is no consensus on an optimal therapeutic strategy [5, 20–23].

ATP-dependent chromatin remodeling plays a critical role in cell differentiation through control of transcriptional programs. When disrupted, these programs result in abnormal gene expression that creates therapeutically targetable oncogenic dependencies [24]. For example, in BRG1-deficient non-small cell lung cancers, BRM has been identified as a candidate synthetic lethal target [25, 26]. Similarly in BRG1-deficient small cell lung cancer, MYC-associated factor X (MAX) was identified as a synthetic lethal target [27]. In ARID1A-mutated OC, inhibition of DNA repair proteins PARP and ATR, and the epigenetic factors EZH2, HDAC2, HDAC6 and BRD2 have all shown therapeutic promise [28]. In SCCOHT, therapeutic vulnerabilities to receptor tyrosine kinase inhibitors [29], EZH2 inhibitors [30–32], HDAC inhibitors [33], bromodomain inhibitors [34], and CDK4/6 inhibitors [35, 36] have also been identified. Importantly, correlations between SWI/SNF mutations and responses to immune checkpoint inhibitors have also been observed [37]. In renal cell carcinoma, patients carrying mutations in bromodomain-containing genes (PBRM1 and BRD8) showed exceptional response to the anti-CTLA-4 antibody Ipilimumab [38]. A CRISPR screen to identify genes involved in anti-PD-1 resistance identified three SWI/SNF complex members as important determinants in melanoma [39]. A moderate response to anti-PD-1 treatment was also reported in a cohort of four SCCOHT patients expressing PD-L1 [40], suggesting that the low tumor mutation burden is not a limitation for checkpoint immunotherapy. OCCC models have also recently been described to be responsive to checkpoint inhibition in combination with HDAC6 inhibitors, particularly in the ARID1A-deficient setting [41]. In a Phase II clinical trial testing Nivolumab in platinum-refractory OCs, one of the two OCCC patients achieved a complete response [42].

These data suggest that novel treatment approaches and combinations should be adopted to develop targeted therapies against SWI/SNF-mutant ovarian cancers.

Lysine-specific histone demethylase 1 (LSD1/KDM1A) is an epigenetic enzyme that can either repress target gene expression by demethylating mono- or di-methylated histone H3 lysine 4 (H3K4me1/2) or activate targets by removing repressive H3K9me1/2. LSD1 is implicated in tumorigenesis and progression of many cancers and high LSD1 levels frequently correlate with aggressive cancer features [43–45]. LSD1 also promotes tumor progression through demethylation of non-histone substrates such as p53, E2F1, and DNMT1 in addition to MYPT1, a regulator of RB1 phosphorylation [46–50]. Further, recent studies indicate that LSD1 ablation can trigger anti-tumor immunity through induced expression of endogenous retroviruses (ERVs) and reduced expression of the RNA-induced silencing complex (RISC). The accumulation of double-stranded RNA (dsRNA) results in the stimulation of interferon (IFN) β -dependent immunogenic responses [51]. These studies also show that LSD1 inhibition overcomes resistance to checkpoint blockade therapy *in vivo* by increasing tumor immunogenicity and T-cell infiltration [51–53]. Moreover, several studies have shown direct interaction between LSD1 and SWI/SNF complexes in a variety of cancer types. For instance, in glioma, LSD1 is part of a co-repressor complex containing TLX, RCOR2, and the SWI/SNF core complex. Together, this co-repressor complex regulates stem-like properties of glioma initiating cells (GICs) [54]. When LSD1 is associated with SWI/SNF, CoREST, HDAC1/2, and DNMTs, it regulates gene expression in the neural network underlying neurodegenerative diseases and brain tumors [55]. In breast cancer, LSD1 associates with the SWI/SNF subunit SMARCA4 to form a hormone-dependent transcriptional repressor complex [56]. A similar association is required for endogenous Notch-target gene expression in T-ALL cells [57]. These findings suggest LSD1 as an important therapeutic target in cancers driven by SWI/SNF mutations.

In this study, we explored the therapeutic potential of SP-2577 (Seclidemstat), a potent reversible LSD1 inhibitor currently in Phase I clinical trials for Ewing Sarcoma (NCT03600649) and for advanced solid tumors (NCT03895684), to promote anti-tumor immunity and T-cell infiltration in SWI/SNF-mutant OC. Our findings show that SP-2577 promotes ERV expression, activates the dsRNA-induced IFN pathway, and enhances T-cell infiltration in SCCOHT. Treatment with SP-2577 also promotes PD-L1 expression, and thus can potentially overcome resistance to anti-PD-1 therapy in SCCOHT. Finally, the efficacy of SP-2577 to promote T-cell infiltration is not exclusive to SCCOHT. We observed similar effects in other SWI/SNF-mutated OCs, such as ARID1A-mutant OCCC. Our data strongly suggest LSD1 as a potential therapeutic target in SCCOHT and provides preclinical evidence supporting the combinatorial use of SP-2577 with anti-PD-L1 for SWI/SNF-mutation-dependent OCs.

Materials and methods

Cell culture

SCCOHT cell lines BIN67 and SCCOHT-1 (generously donated by Dr. William Hendricks, TGen) were cultured in RPMI Medium 1640 with L-Glutamine (Gibco; catalog no. 11875–093) supplemented with 10% FBS (Gibco; catalog no. 16000069) and 1% penicillin/streptomycin (Gibco; catalog no. 15140163). SCCOHT cell line COV434 (generously donated by Dr. William Hendricks, TGen Phoenix AZ), OCCC cell line TOV21G (ATCC), and the doxycycline-inducible COV434 pIND20 BRG1-2.7 and TOV21G pIND20 ARID1A (generously donated by Dr. Bernard Weissman, University of North Carolina) were cultured in DMEM (Gibco; catalog no. 11965–118) supplemented with 10% TET free FBS (Corning; catalog no. 35-075-CV) and 1% penicillin/streptomycin. All cells were maintained at 37°C with 5% CO₂

in a humidified incubator. All cell lines were routinely monitored for mycoplasma contamination and STR profiled for cell line authentication.

The LSD1 inhibitor screening assay

The LSD1 inhibitor screening assay (Cayman Chemical; catalog no. 700120) was performed as previously described [58]. Briefly, SP-2577 and SP-2513, (Salarius Pharmaceuticals, Houston TX), were diluted to 20X the desired test concentration in 100% DMSO (Millipore Sigma; catalog no. D2650-100ML) and 2.5 μ L of the diluted drug sample was added to a black 384-well plate. The LSD1 enzyme stock was diluted 17-fold with assay buffer and 40 μ L of the diluted LSD1 enzyme was added to the appropriate wells. Substrate, consisting of horseradish peroxidase, dimethyl K4 peptide corresponding to the first 21 amino acids of the N-terminal tail of histone H3, and 10-acetyl-3, 7-dihydroxyphenoxazine was then added to wells. Resorufin was analyzed on an Envision plate reader with an excitation wavelength of 530 nm and an emission wavelength of 595 nm.

Cell viability assay

Cells were seeded in 96-well plates in triplicate at a density of 500–2000 cells per well depending on the growth curve of each cell line. After 24 h, cells were treated with DMSO, the LSD1 inhibitor SP-2577 or the analog SP-2513 at increasing concentrations (0.001 to 10 μ M). Cell viability was assessed with CellTiter-Glo (Promega; catalog no. G7573) 72 h after treatment and IC_{50} were calculated using GraphPad Prism v. 8.0. Absorbance values were normalized to DMSO-treated controls.

Organoid generation

SCCOHT cell lines (BIN67, SCCOHT-1, COV434) and the OCCC cell line TOV21G were seeded at 5000 cells per well in 96-well ultra-low attachment spheroid microplates (Corning; catalog no. 4591) in 40 μ L of appropriate phenol red free medium (DMEM, Thermo Fisher Scientific Catalog No. 21063045; RPMI, Thermo Fisher Scientific catalog no. 11-835-030) containing 1.5% growth factor reduced matrigel (Corning; catalog no. 354230). The plates were then centrifuged at 2000 rpm for 2 mins at RT. Cells were cultured for 72 h with 5% CO_2 in a humidified incubator to generate spheroids for use in immune infiltration assays.

Immune infiltration assay

SP-2577/SP-2513 conditioned media. The SCCOHT and OCCC cell lines were seeded in T-25 tissue culture treated flasks (Genesee Scientific; catalog no. 25–207) at 3×10^5 cells in 5mL of the appropriate phenol red free complete growth medium. After 48 h, at 70–80% confluency, the cells were treated with 3 μ M or 1 μ M of SP-2577 or SP-2513. After 72 h, the media was collected from the flasks and stored at $-80^\circ C$ until use in the infiltration assays.

Labeling of PBMCs. Human peripheral blood mononuclear cells (PBMC) (Lonza; catalog no. CC-2702) were maintained in CTS OpTmizer T Cell expansion SFM (Thermo Fisher; catalog no. A1048501) in a T-75 suspension flask (Genesee Scientific; 25–214) for 24 h at $37^\circ C$. After 24 h, cells were collected and washed with PBS (Gibco; catalog no. 10010031) and counted. Approximately 2.5×10^6 PBMCs were labeled with Molecular Probes Vybrant CM-Dil Cell Labeling Solution (RFP) (Thermo Fischer; catalog no. C7000) by incubating the PBMCs with a 2 μ M solution of Molecular Probes Vybrant CM-Dil for 45 min at $37^\circ C$ in the dark and then for an additional 15 min at $4^\circ C$. After the incubation, cells were washed with PBS twice and resuspended in the appropriate complete growth medium.

Checkpoint blockade. The following monoclonal blocking antibodies (final concentration 10 $\mu\text{g}/\text{mL}$) were used for checkpoint blocking on tumors as well as T cells: functional grade PD-L1 (29E.2A3) and CTLA-4 (BN13) (Bioxcell, USA). In brief, 2×10^6 PBMCs were treated with 10 $\mu\text{g}/\text{mL}$ of α -CTLA-4 antibody and incubated at 37°C incubator for 45 min on shaker. Then, the cells were washed in serum free media and stained with Molecular Probes Vybrant CM-Dil Cell Labeling Solution as mentioned above. Alternatively, COV434 pIND 20 BRG1-2.7 and TOV21G pIND20-ARID1A tumor organoids were incubated with 10 $\mu\text{g}/\text{mL}$ of α -PD-L1 antibody and incubated at 37°C for 1 h. The media containing α -PD-L1 was carefully removed with a pipette and replaced with fresh conditioned media.

Immune infiltration and imaging. 150 μL of SP-2577 conditioned medium was added to each well containing a spheroid. A 5 μm HTS Transwell 96-Well Permeable Support receiver plate (Corning, catalog no. 3387) was placed on each ultra-low attachment spheroid microplate (Corning) to allow for PBMC infiltration into the tumoroids. Molecular Probes Vybrant CM-Dil -stained PBMCs were then seeded into inserts at 5×10^5 cells/well to ensure tumoroid:PBMC cell ratio of 1:10. After 48 h, inserts were removed, and organoid microplates were analyzed by 3D Z-stack imaging and morphometric analysis with Cytation 5 software to quantify the lymphocyte infiltration.

qPCR

COV434, COV 434 pIND20 BRG1-2.7, BIN67, and SCOOHT-1 cells were seeded at a 1×10^6 cells in 2 mL of appropriate medium in 6-well tissue culture treated plates (Genesee Scientific, catalog no. 25–105). After 24 h, cells were treated with 1 μM and 3 μM of SP-2577 as well as 3 μM of SP-2513 for 72 h. DMSO was used as negative control. To quantify gene expression, total RNA was extracted (Qiagen RNeasy Mini Kit; catalog no. 74106) and quantified by spectroscopy (Thermo Scientific; Nanodrop ND-8000). Samples were then reverse transcribed to cDNA using a high capacity cDNA reverse transcription kit (Thermo Scientific, catalog no. 4368814) and the MJ Research thermal cycler. cDNA was amplified, detected, and quantified using SYBR green reagents (Thermo Scientific; catalog no. A25778) and the ViiA 7 Real-Time PCR System (Applied Biosystems). Data were normalized to GAPDH expression. A list of primers used in this study are provided in [S2 Table](#).

Fluorescent staining and imaging of organoids

Organoids grown in Matrigel were initially fixed in 4% PFA (Millipore Sigma catalog no. 47608) for 1.5 h. After PBS washing, organoids were embedded in HistoGel Specimen Processing Gel (Thermo Fisher Scientific catalog no. HG-4000-012), processed with an automated tissue processor (Sakura Tissue-Tek VIP), and embedded into a paraffin block (Tissue-Tek TEC). Samples were sectioned at 4 μm onto poly-L-lysine coated slides (Sigma-Aldrich; catalog no. P4707) and air-dried at RT over-night for any subsequent immunofluorescence staining. All slides for fluorescence were deparaffinized and antigen retrieved in pH 6 citrate buffer for a total of 40 min. After protein blocking, nuclei were stained with DAPI (Abcam; catalog no. ab104139). Infiltrating PBMCs were pre-stained with Molecular Probes Vybrant CM-Dil as described above. Imaging was performed on a Zeiss LSM880 fluorescent microscope with Zen Black software.

Flow cytometry and antibodies

A digestion step was performed for the harvest and characterization of lymphocytes infiltrated into the organoids. Briefly, organoids were removed from culture insert after immune infiltration experiments, washed with PBS twice to eliminate the PBMCs, which are not inside the

organoids, and incubated with Gentle Cell Dissociation reagent (Stem Cell Technologies; catalog no. 07174) for 2 min at RT. Next, the organoids were mechanically disrupted by pipetting. After complete disaggregation, single cell suspensions were dissolved in Cell Staining buffer (Biolegend, catalog no. 420201) and incubated at 4°C for 10 min with antibody staining.

Cells were stained with anti-human CD45 (eBioscience; catalog no. 17-0459-42), CD3 (Biolegend; catalog no. 344840), CD8 (Biolegend; catalog no. 344709), CD4 (Biolegend; catalog no. 300505), CD56 (BD Pharmingen; catalog no. 556647) and CD19 (Biolegend; catalog no. 363005) antibodies. Cell viability was assessed by negative live/dead antibody staining (Miltenyi Biotech; catalog no. 130-109-816). Analysis was performed on a BD FACS Canto II (BD Biosciences). BV421⁺ and single cells were gated out, followed by CD45⁺ cell selection. Analysis of CD3, CD8, CD4, CD56, and CD19 lymphocyte populations was performed with FlowJo software (Tree Star Inc.)

Western blotting

COV434 pIND20 BRG1-2.7 cells were plated in 6-well tissue culture plates at a density of 5×10^5 cells per well and left to adhere overnight. Once adherent, cells were treated with 1 μ M doxycycline (Millipore Sigma, catalog no. 10592-13-9) daily for 8 days. Cells were harvested daily and lysates were produced with EpiQuik Nuclear Extraction Kit (EpiGentek, catalog no. OP-0002-1). Nuclear proteins were resolved by SDS-PAGE and immunoblotted for BRG1/SMARCA4 expression (Abcam, catalog no.118558). Given the high molecular weight of the protein, LSD1 was used to normalize the total protein loaded in the gel (Cell Signaling Technology, catalog no: 4218). Densitometry analysis was performed with LiCor Odyssey imaging software and Prism GraphPad.

Analysis of TCGA dataset

Pan-Cancer expression of KDM1A (LSD1). All TCGA PanCancer Atlas data was downloaded from cBioPortal. Median RNA sequencing expression data for each cancer type was extracted and imported into RStudio. KDM1A expression data was queried and plotted using the `boxplot` function within RStudio. The cancer type acronyms used are from TCGA Pan-Cancer Atlas with the full cancer type key provided in [S1 Table](#).

KDM1A expression in wild-type and mutant SWI/SNF cancers across the TCGA Pan-Cancer Atlas. KDM1A expression with SWI/SNF mutational data was generated using the `query` function on the cBioPortal website. The dataset selected was TCGA PanCancer Atlas studies (10967 samples) and the genes queried were: SMARCA4, ARID1A, SMARCB1, SMARCC1, and KDM1A. Downloaded from cBioPortal were the sample matrix list of all samples with mutations and the mRNA expression (RSEM batch normalized from Illumina HiSeq_RNASeqV2) of the 5 genes listed above. Samples were removed from the analysis that had only KDM1A mutations, KDM1A deletions, no profiling of SWI/SNF genes, or did not have expression data. The samples were separated into two groups, SWI/SNF mutant (1338 samples) and SWI/SNF wild-type (8448 samples). Boxplots were generated using GraphPad Prism v 8.0 and significance was calculated using Mann-Whitney non-parametric independent test in RStudio with a p-value < 0.0001.

U-plex MSD analysis

MSD analysis was performed following the manufacturer's protocol (Meso Scale Discovery). Briefly, conditioned media (CM) from SP-2577 and DMSO treated cells were collected and centrifuged at 1500 RPM for 5 min at 4°C to eliminate cell debris. CM was then concentrated using Centricon 3 KDa (Merck Millipore; catalog no. UCF800396) and 25 μ L of the resulting

CM was added to each well in the MSD plate (Meso Scale Discovery KIT no. K15067L-2) and analyzed using Discovery Workbench 4.0 software.

Statistical analysis

Two-tailed student's paired T-tests with 95% confidence intervals were performed using GraphPad Prism v 8.0. Symbols for significance: NS, non-significant; * = $p < 0.05$; ** = $p < 0.01$; **** = $p < 0.0001$. All the *in vitro* experiments were performed in triplicate and repeated at least three times.

Results

LSD1 is highly expressed in SWI/SNF-mutant cancers and the LSD1 inhibitor SP-2577 inhibits SWI/SNF-mutation-dependent tumor cell proliferation

Analysis of the TCGA Pan-Cancer dataset showed that LSD1 is highly expressed in the majority of human cancers (Fig 1A, S1 Table), including in SWI/SNF-mutant tumors (Fig 1B) [59, 60]. To determine the effects of SP-2577 on SWI/SNF-mutant cell viability, we performed drug-dose-response (DDR) studies with 72 h CellTiterGlo viability endpoints in SCCOHT (SMARCA4^{-/-}), OCCC (ARID1A^{-/-}), lung (SMARCA4^{-/-}), kidney (SMARCB1^{-/-}), and colorectal cancer cell lines (SMARCA4^{-/-}). All cell lines were sensitive to SP-2577 treatment and showed sub-micromolar IC₅₀ (Table 1). Cell lines treated with SP-2513, an analog of SP-2577 that poorly inhibits LSD1 enzymatic activity (Table 2), showed significantly higher 72 h IC₅₀ that ranged from 3.5 to 10 μ M (Table 1).

Inhibition of LSD1 by SP-2577 promotes ERV expression and induces expression and release of effector T cell-attracting chemokines in conditioned medium

Inhibition of LSD1 activity has been suggested to enhance anti-tumor immunity through activation of ERVs and production of dsRNA, followed by activation of an IFN- β -dependent immune response [51]. To investigate whether SP-2577 treatment could promote a similar response in SCCOHT tumors, we analyzed the expression of ERVL, HERVK, and IFN- β in

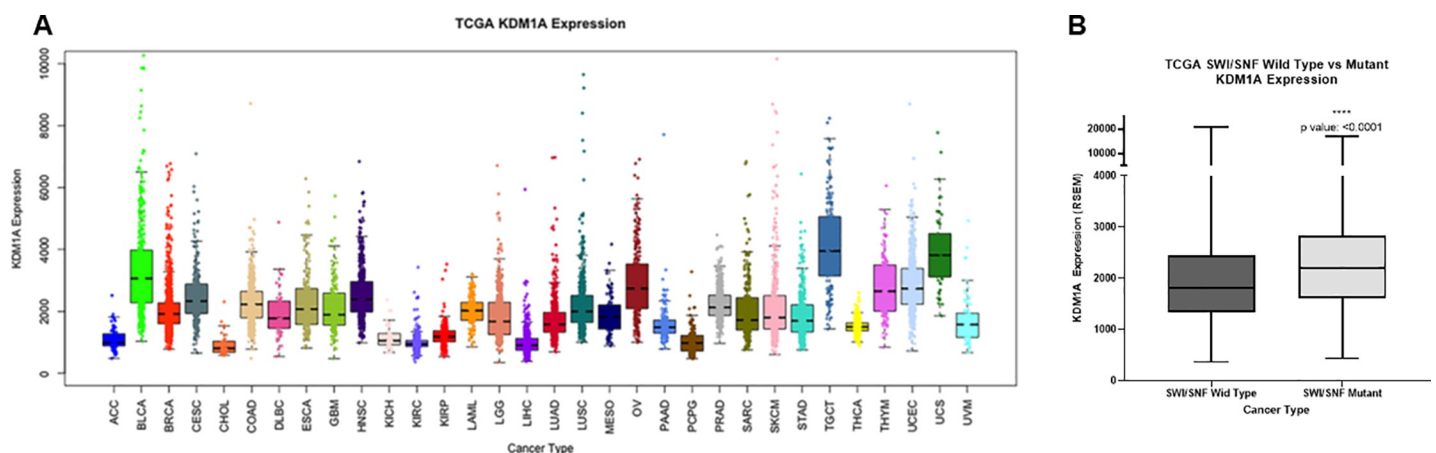


Fig 1. LSD1 expression in tumors and SP-2577 toxicity in SWI/SNF mutated tumors. (A) TCGA analysis for LSD1 expression in different human cancers. The cancer type acronym to full cancer type key from TCGA PanCancer Atlas is in S2 Table. (B) TCGA analysis for LSD1 expression in SWI/SNF-mutated tumors.

<https://doi.org/10.1371/journal.pone.0235705.g001>

Table 1. Cytotoxicity of SP-2577 and SP-2513 in SWI/SNF-mutated cancer cell lines. Cell viability was evaluated after 72 h treatment with the drugs by Cell Titer Glow assay.

Table 1: Viability assay				
Cancer type	Cell line	SWI/SNF mutation	Drug IC ₅₀ (μM)	
			SP-2577	SP-2513
SCCOHT	COV434	SMARCA4	0.529	9.985
SCCOHT	BIN67	SMARCA4	0.417	10
SCCOHT	SCCOHT-1	SMARCA4	1.098	3.65
OCCC	TOV21G	ARID1A	0.203	24.54
Ovary ADC	SKOV3	SMARCC1	0.013	---
Lung ADC	A427	SMARCA4	0.1422	---
Lung ADC nscl	H522	SMARCA4	2.819	---
Lung ADC	A549	SMARCA4	0.248	---
Lung ADC nscl	H1299	SMARCA4	0.212	---
Kidney Rhabdoid	G401	SMARCB1	0.3874	---
Kidney renal leiomyoblast	G402	SMARCB1	1.179	---
CRC	HCC15	SMARCA4	0.117	---

<https://doi.org/10.1371/journal.pone.0235705.t001>

SCCOHT cell lines (COV434, BIN 67 and SCCOHT-1) treated with SP-2577. After 72 h treatment with 3 μM SP-2577, quantitative PCR (qPCR) analysis showed that SP-2577 significantly upregulated the expression of ERVs, IFN-β, and interferon-stimulated gene CXCL10, suggesting activation of an IFN-dependent immune response (Fig 2A). Recently, it has been shown that LSD1 inhibition in triple negative breast cancer cell lines induces expression of CD8⁺ T cell-attracting chemokines, including CCL5, CXCL9, and CXCL10 [61]. The expression of these genes along with PD-L1 was shown to have increased H3K4me2 levels at proximal promoter regions [61] in response to LSD1 inhibition. To determine whether SCCOHT cell lines release CD8⁺ T cell-attracting chemokines after LSD1 inhibition, we analyzed the conditioned media from COV434 cells treated with SP-2577 for 72 h. Our U-PLEX MSD data showed that treatment with SP-2577 stimulated chemokine secretion in COV434 culture medium (Fig 2B). Further, secretion of cytokines, including IL-1β, IL-2, and IL-8, were also observed in the treated conditioned medium. Together, these data suggest that SP-2577 may play a role in the promotion of anti-tumor immunity.

SP-2577 promotes lymphocyte infiltration in 3D culture of SCCOHT cell lines

To examine whether SP-2577-dependent cytokine and chemokine secretion could enhance lymphocyte trafficking and tumor infiltration, we carried out an *ex vivo* migration/infiltration assay. SCCOHT cell lines COV434, BIN67, and SCCOHT-1 were grown in low concentration matrigel to form 3D organoids as described in Methods. To prevent SP-2577 cytotoxic damage from directly impacting cell viability, the organoids were cultured in conditioned media from SCCOHT cell lines collected 72 h post-treatment with SP-2577. At this time point, there was

Table 2. Inhibition of LSD1 enzymatic activity of SP-2577 and SP-2513 measured by Resorufin assay in a cell-free system.

Table 2: LSD1 screening biochemical assay	
Drug	IC ₅₀ (μM)
SP-2577	0.013
SP-2513	>1

<https://doi.org/10.1371/journal.pone.0235705.t002>

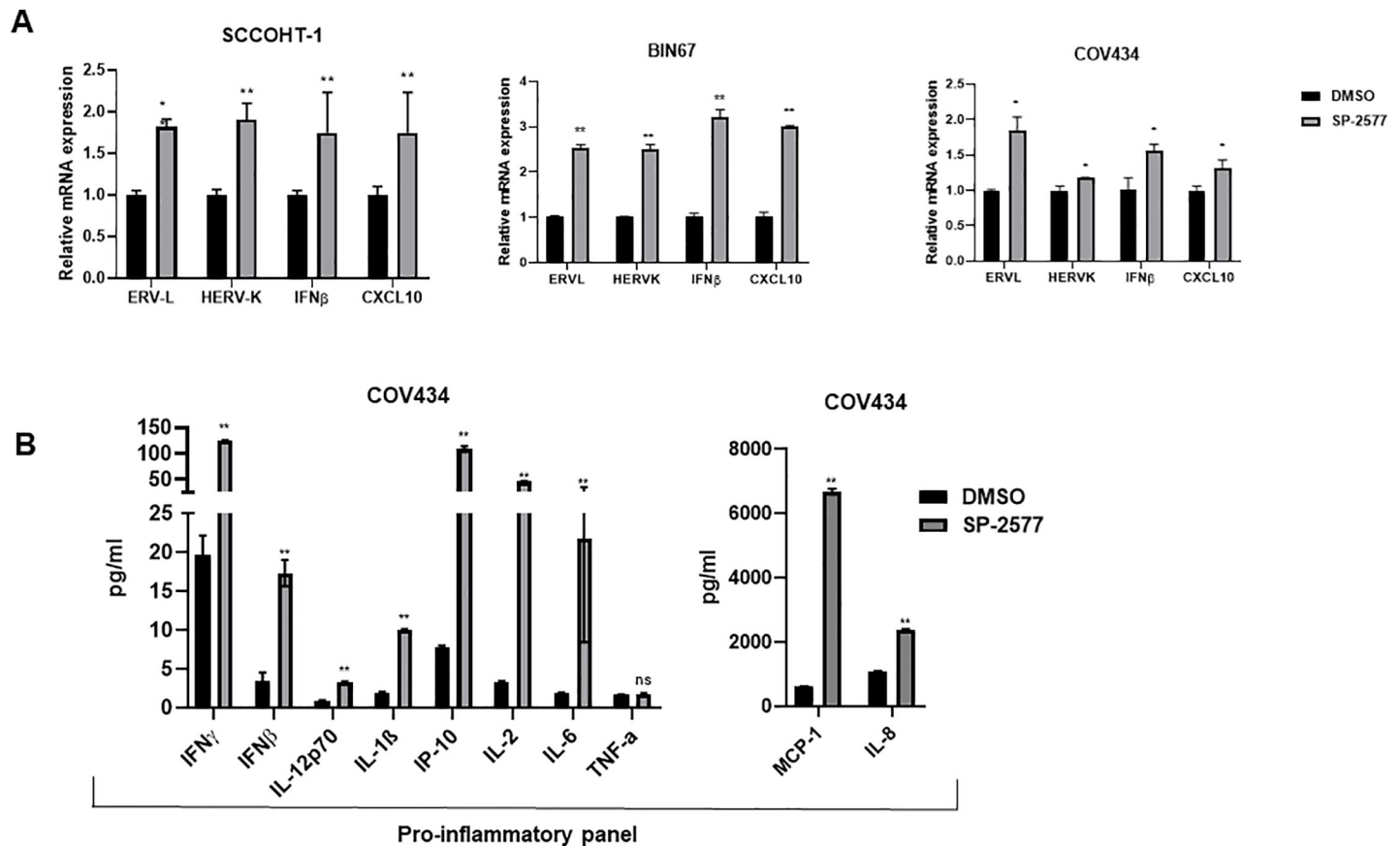


Fig 2. SP-2577 promotes ERVs expression and activation of IFN β pathway in SCCOHT cell lines. (A) qPCR analysis of SCCOHT cell lines SCCOHT-1, BIN67, and COV434 after 72 h of SP-2577 treatment showing increased expression of ERVs and IFN pathway cytokines. (B) MSD panel of chemokines and cytokines from SCCOHT COV434 cell conditioned media in the presence or absence of SP-2577 for 72 h. * = $p < 0.05$, ** = $p < 0.01$.

<https://doi.org/10.1371/journal.pone.0235705.g002>

no drug present in the conditioned medium. Migration and infiltration of lymphocytes was determined utilizing RFP-stained human allogeneic PBMCs. PBMCs were added to organoid cultures and migration toward the organoids was assessed by 3D Z-stack imaging and morphometric analysis (Cytation 5, BIOTECK). SP-2577 promoted PBMC infiltration in organoids more efficiently than the less active analog SP-2513 (Fig 3A). Immunofluorescence analysis further demonstrated the presence of stained PBMCs in the sectioned organoids that were treated with SP-2577 conditioned medium, while they were absent in organoids cultured in SP-2513 or DMSO-conditioned medium (Fig 3B). Finally, to determine the dependency of PBMC infiltration on SP-2577, we performed *ex vivo* migration/infiltration studies with higher concentrations of the LSD1 inhibitor (3–0.03 μ M). SP-2577 induced PBMC infiltration into the SCCOHT organoids in a dose-dependent manner (Fig 3C). Together, these observations suggest that the chemokines and cytokines secreted by SCCOHT cells in response to SP-2577 treatment promote the migration and infiltration of PBMCs in tumor organoids.

Treatment with SP-2577 promotes infiltration of CD8⁺ T cells into SCCOHT organoids

Next, we investigated which lymphocyte populations infiltrated the SCCOHT organoids after SP-2577 treatment *in vitro*. Flow cytometry analysis of the dissociated COV434 organoids

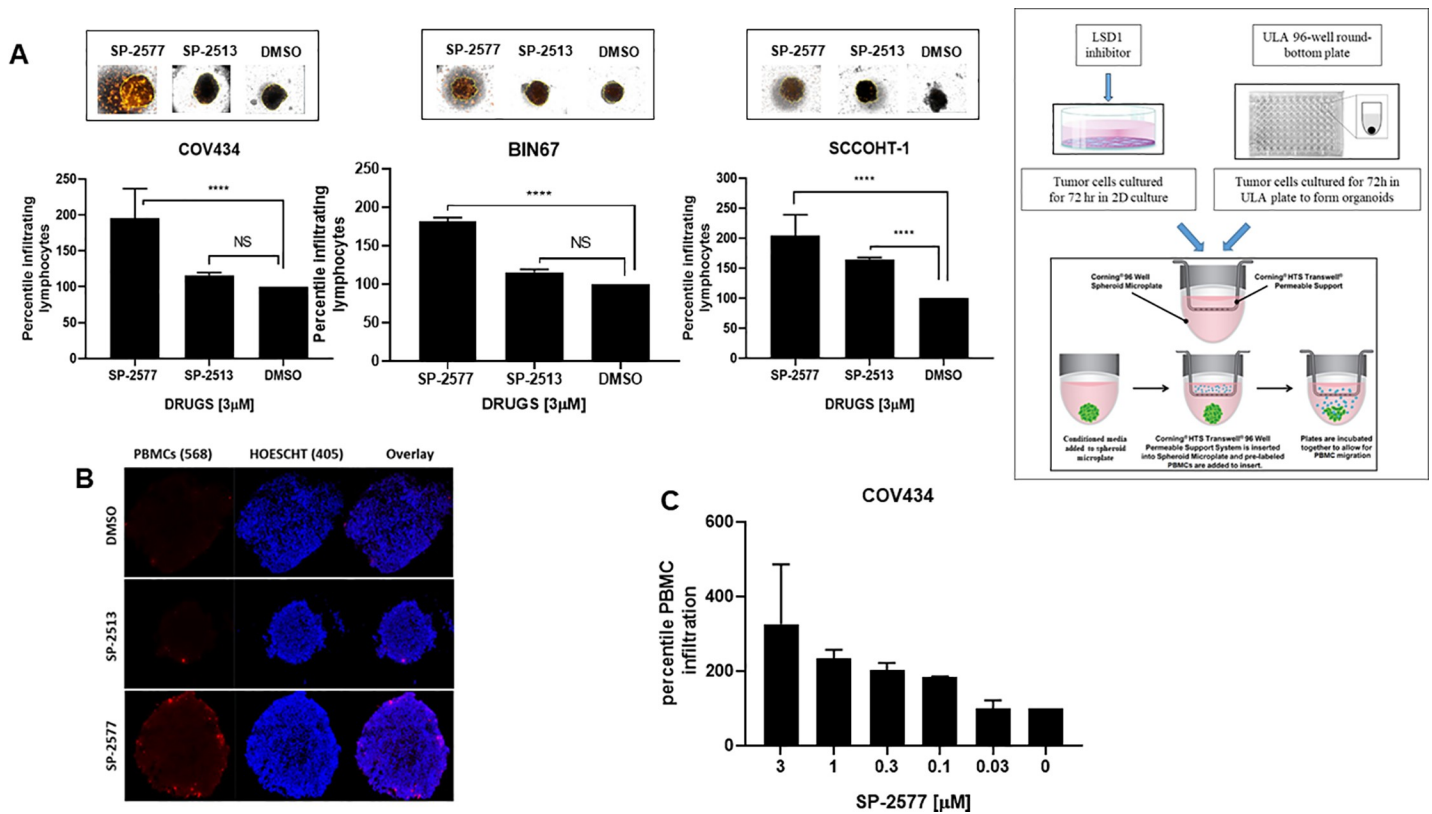


Fig 3. SP-2577 promotes lymphocyte infiltration in SCCOHT tumor organoids. (A) Immune infiltration assay in SCCOHT organoids imaging analysis. COV434, BIN67 and SCCOHT-1 derived-organoids were incubated with conditioned medium pretreated with 3 μM SP-2577, SP-2513, or DMSO in the presence of RFP-tagged PBMCs. After 48 h, the levels of lymphocyte infiltration were measured by z-stack analysis by Cytation 5 imaging. P values for COV434 = <0.0001, BIN67 = 0.0016, and SCCOHT-1 = 0.0196. Right panel: Experimental design (B) IF analysis: RFP-tagged lymphocyte infiltration in SCCOHT organoid microsections was assessed by analysis of RFP levels on confocal scope after 48 h co-culture in presence of SP-2577 or SP-2513 conditioned medium. (C) Immune infiltration assay of COV434 cells treated with increased concentration of SP-2577 for 48 h. The amount of lymphocyte infiltration correlates with SP-2577 dose.

<https://doi.org/10.1371/journal.pone.0235705.g003>

showed the predominance of CD3⁺ T lineage cells (Fig 4Ai and 4Bi). The percentile of CD8⁺ T cell in SP-2577 treated organoids was significantly enriched (Fig 4Bii; p-value <0.0001) in comparison to those untreated (Fig 4Aii). Similarly, CD4⁺ and CD4⁺CD8⁺ Double Positive T cells levels increased significantly after treatment with SP-2577 (Fig 4Aii and 4Bii). CD56⁺ NKT cells and CD19⁺ B cells were present in small numbers compared to the total CD45⁺ cell population. CD56⁺ NKT cells increased approximately 15-fold after treatment with SP-2577 (Fig 4Aiii and 4Biii), while CD19⁺ B cells decreased by approximately 3-fold (Fig 4Aiv and 4Biv). All together, these data suggest that treatment with SP-2577 promotes T cells and NKT cells infiltration into the tumor, which subsequently leads to tumor cytotoxicity.

Inhibition of LSD1 by SP-2577 induces expression of PD-L1

LSD1 expression has been shown to negatively correlate with expression of immune-related genes, including PD-L1 [61]. Further, LSD1 has been shown to play a critical role in epigenetic silencing of the expression of PD-1 [62], and LSD1 inhibition results in increased expression of PD-L1 in tumor cells [51, 61]. To investigate the effect of SP-2577-dependent LSD1 inhibition on the expression of PD-L1 in SCCOHT, we treated organoids generated with the isogenic COV434 cell line, engineered to express BRG1 upon treatment with doxycycline (hereby identified as COV434 pIND 20 BRG1-2.7) [29], with 3 μM SP-2577 and performed qPCR

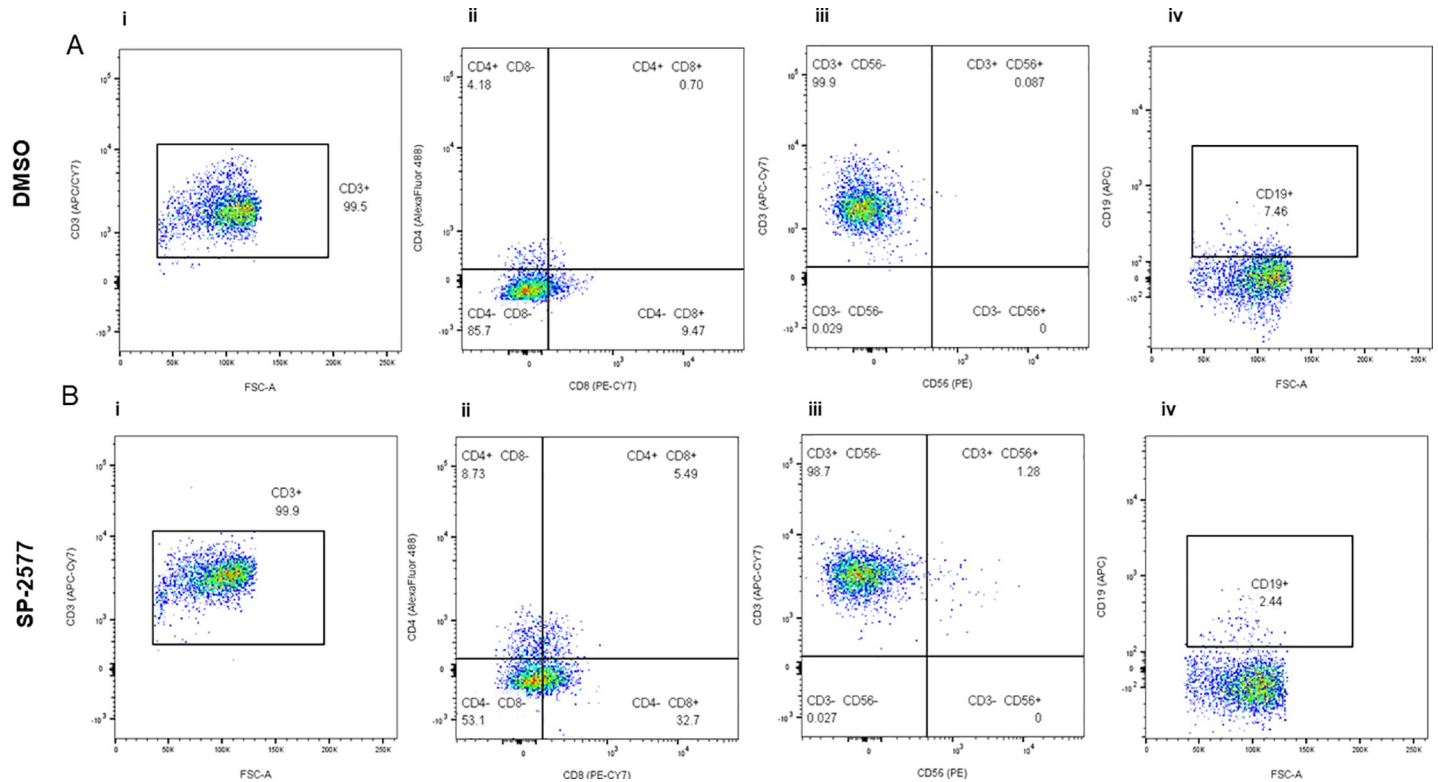


Fig 4. Flow cytometry analysis of the COV434 organoids after lymphocyte infiltration assay. COV434 organoids were dissociated and the infiltrated lymphocytes were stained with different markers and analyzed by flow cytometry as described in 'Materials and Methods'. Panel A and B are showing the status of lymphocytes infiltrated in DMSO control organoids and SP-2577 treated organoids, respectively, in the representative dot plots. **(Ai and Bi)** The dot plots showed the CD3⁺ population in CD45⁺ gated lymphocytes. **(Aii and Bii)** The status of CD4⁺ and CD8⁺ T cells gated on CD3⁺ cells are presented in different quadrants. **(Aiii and Biii)** Percentage of CD56⁺ NK in CD3⁺ cells are presented with quadrant statistics. **(Aiv and Biv)** The status of CD19⁺ B cells are shown in CD3⁺ cells.

<https://doi.org/10.1371/journal.pone.0235705.g004>

analysis for PD-L1 expression. As shown in Fig 5A, we observed a significant increase in PD-L1 expression after drug treatment (p-value<0.0001; Fig 5A, left panel). Next, we tested if checkpoint blockade could amplify the immune cell infiltration effect in the presence of SP-2577 in immune-organoids. As shown in Fig 5B, co-treatment of low doses (100 nM) of SP-2577 with α -PD-L1 significantly increased lymphocyte infiltration (p-value<0.05). Moreover, the combination of α -PD-L1 and α -CTLA-4 was able to significantly enhance the infiltration of PBMCs in the SP-2577-treated COV434 pIND 20 BRG1-2.7 organoids (p-value<0.01; Fig 5B).

SMARCA4 re-expression in SCCOHT cell lines blocks lymphocyte infiltration

Although SCCOHT is characterized by low tumor mutation burden, recent studies have indicated that the tumor microenvironment of SCCOHT is similar to other immunogenic tumors that respond to checkpoint blockade [37, 40, 63], suggesting that mutations in the subunits of the SWI/SNF complex may contribute to immunotherapy sensitivity. We questioned whether the restoration of SWI/SNF functionality in SCCOHT would affect the lymphocyte trafficking and tumor infiltration observed with SP-2577 treatment. To investigate this hypothesis, we used the isogenic COV434 pIND20 BRG1-2.7 where SMARCA4 (*BRG1*) is expressed under a doxycycline inducible system [29]. Western blotting and qPCR analysis confirmed the expression of SMARCA4 in doxycycline-treated cells (Fig 6A, Fig 6B and S1 Raw images).

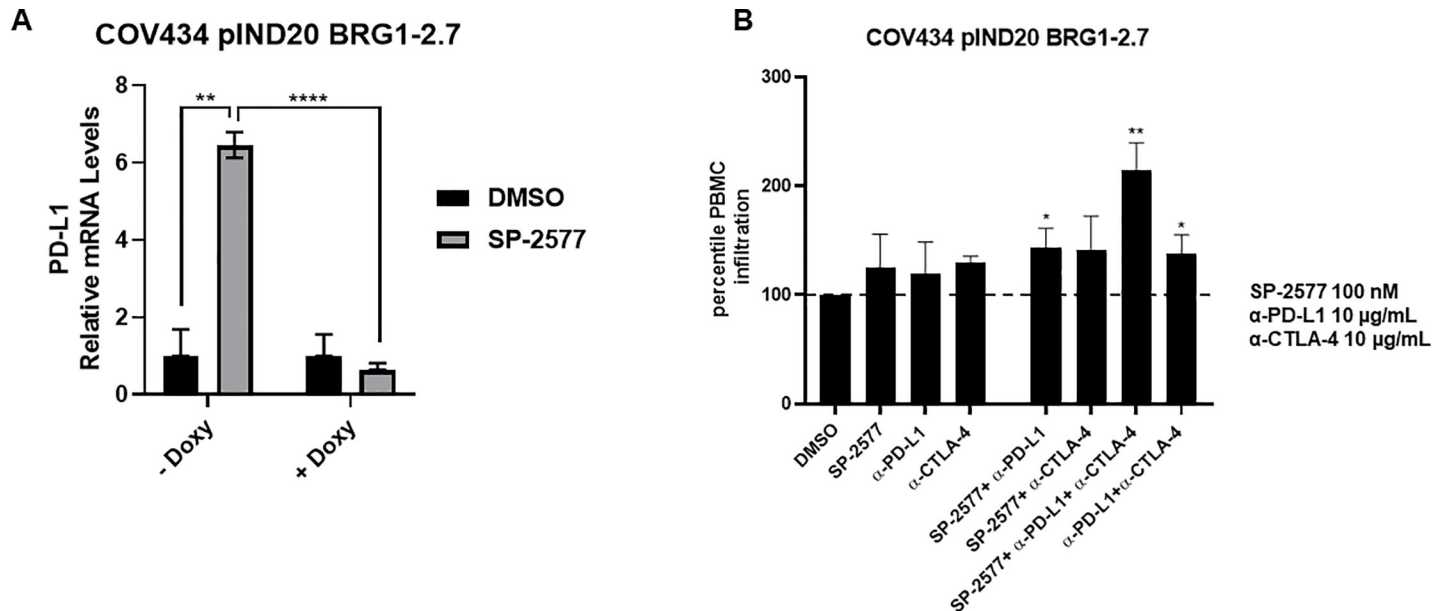


Fig 5. SP-2577 promotes PD-L1 expression and rescues checkpoint inhibition sensitivity in SCCOHT COV 434 pIND 20 BRG1-2.7 cell line. (A) RT-PCR analysis of COV434 pIND 20 BRG1-2.7 cells after SP-2577 treatment shows increase of PD-L1 expression levels, which are lost after doxycycline treatment. (B) Co-treatment of COV434 pIND 20 BRG1-2.7 organoids with SP-2577 and anti-PD-L1 antibodies or lymphocytes treated with anti-CTLA-4 antibodies showed an increase in lymphocyte infiltration as checked after 48 h.

<https://doi.org/10.1371/journal.pone.0235705.g005>

SMARCA2 (*BRM*), which is normally silent in SCCOHT tumors, was also overexpressed by 14-fold after BRG1 induction (Fig 6B). We observed a significant reduction in the level of infiltrated lymphocytes in SMARCA4 re-expressed organoids after SP-2577 treatment (p -value < 0.05; Fig 6C). Remarkably, expression of endogenous retroviruses elements such as ERVL, HERVK, as well as IFN β and interferon-stimulated gene ISG15 was significantly downregulated in SMARCA4-induced cells after treatment with SP-2577 (Fig 6D) when compared with the not-induced (Fig 2A), while the expression of CXCL10, known to be doxycycline transcription-dependent (64), remained unchanged (Fig 6D). In addition, re-expression of SMARCA4 resulted in downregulation of PD-L1 expression in SCCOHT cell lines (Fig 5A). Lastly, the production and secretion of cytokines and chemokines that were promoted by SP-2577 treatment were negatively affected by the re-expression of SMARCA4 in SCCOHT cells when compared to the control (Fig 6E).

To determine if the reduction of lymphocyte infiltration was solely dependent on the re-expression of SMARCA4, we cultured doxycycline treated COV434 pIND20 BRG1-2.7 organoids with conditioned medium generated from SP-2577-treated parental SCCOHT cells lacking SMARCA4 expression. As shown in Fig 6F, the presence of cytokines and chemokines in SP-2577-treated conditioned medium was not sufficient to overcome the impaired infiltration of lymphocytes in SMARCA4-expressing organoids, suggesting that SMARCA4-dependent epigenetic changes may have altered the immunogenicity of the organoids.

SP-2577 promotes lymphocyte infiltration in ARID1A-deficient cells

To investigate if SP-2577 promotes tumor immune response in other SWI/SNF-mutant tumor types, we performed *ex vivo* migration and infiltration of lymphocytes in ARID1A-deficient OCCC cells. These studies were conducted in isogenic TOV21G pIND 20-ARID1A cells, which re-express ARID1A under the control of doxycycline treatment. As previously observed in SCCOHT cell lines, SP-2577 promotes lymphocyte infiltration in a dose-dependent manner

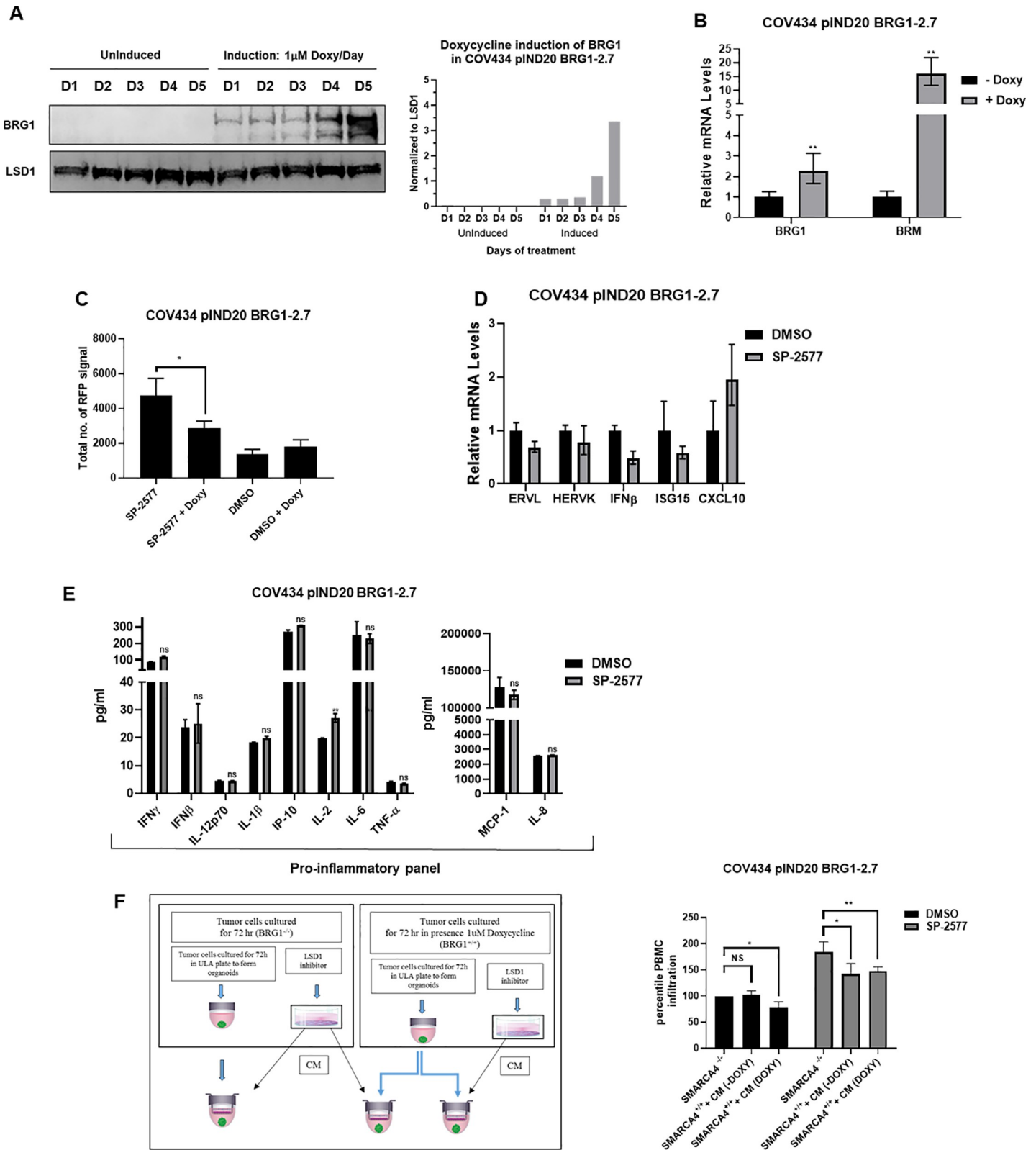


Fig 6. SMARCA4 re-expression in SCCOHT cell lines blocks lymphocyte infiltration. (A) Western blot and densitometry analysis for SMARCA4 expression levels in COV 434 pIND20 BRG1-2.7 after 1 μ M doxycycline daily treatment (D = days). Total protein load was verified by LSD1 expression analysis. (B) RT-PCR for BRG1 and BRM expression levels in COV434 pIND20 BRG1-2.7. Both gene expression increased after SP-2577 treatment. (C) The levels of lymphocyte infiltration are significantly

reduced after SMARCA4 re-expression in COV434 pIND20 BRG1-2.7 (p-value = 0.038). (D) RT-PCR analysis of SMARCA4-induced COV434 pIND20 BRG1-2.7 after 72 h SP2577 treatment shows decrease of ERVs activity and INF expression. (E) MSD analysis of SMARCA4-induced COV434 pIND20 BRG1-2.7 after 72 h SP-2577 treatment shows significant decrease of cyto/chemokines released in medium after treatment. (F) Treatment of SMARCA4-induced COV434 pIND20 BRG1-2.7 organoids with conditioned medium (CM) from SMARCA4-deficient COV434 pIND20 BRG1-2.7 does not affect lymphocyte infiltration suggesting SMARCA4 plays role in immune response. Left panel: Experimental design.

<https://doi.org/10.1371/journal.pone.0235705.g006>

in un-induced TOV21G pIND 20-ARID1A organoids (Fig 7A). Doxycycline-induced re-expression of ARID1A resulted in a significant reduction in infiltration of lymphocytes (Fig 7B). In addition, the combination of α -PD-L1 and α -CTLA-4 significantly enhanced the infiltration of PBMCs in the low dose (300 nM) SP-2577-treated un-induced TOV21G pIND 20-ARID1A organoids (Fig 7C).

Discussion

SWI/SNF complexes have previously been implicated in the regulation of the immune system, particularly in enhancing interferon-stimulated gene (ISG) expression [64] through a STAT-

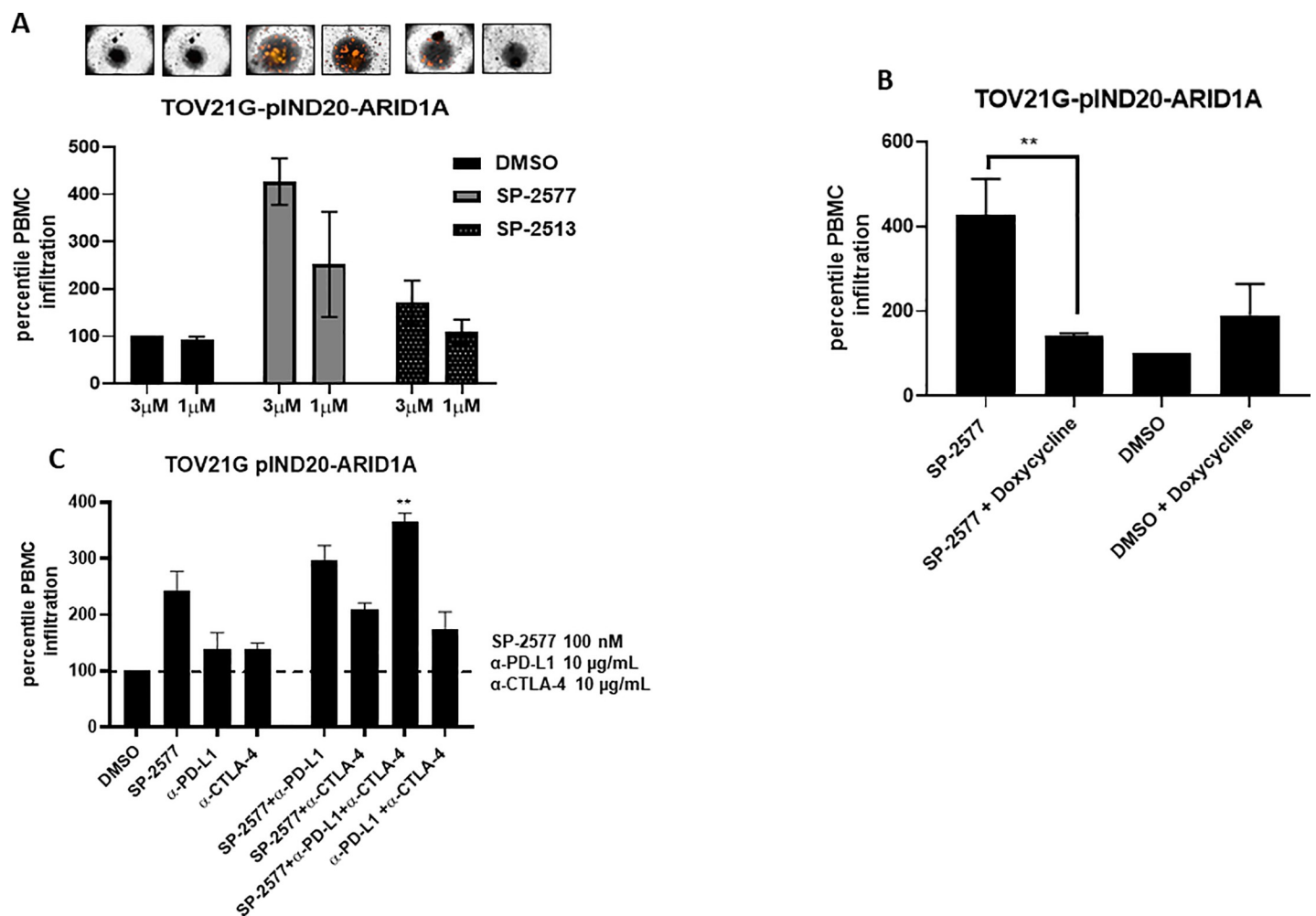


Fig 7. SP-2577 promotes lymphocyte infiltration in ARID1A deficient cells. (A) Amount of lymphocyte infiltration is dependent on SP-2577 treatment in TOV21G pIND20-ARID1A cell lines. (B) Lymphocyte infiltration is significantly reduced in TOV21G pIND20-ARID1A cells after ARID1A re-expression upon doxycycline treatment (p-value = 0.004). (C) Co-treatment of SP-2577 and CTLA-4 antibodies in the immune infiltration assay showed an increase in lymphocyte infiltration in TOV21G-pIND20-ARID1A after 48 h.

<https://doi.org/10.1371/journal.pone.0235705.g007>

dependent mechanism. However, it has been reported that inactivating mutations in SWI/SNF subunits (ARID1A, PBRM1, SMARCB1, and SMARCA4) also sensitize cancer cells to T cell-mediated destruction [37]. SWI/SNF loss-of-function enhances the expression of immune checkpoint regulators and neoantigen presentation [37, 39, 65]. Even monogenic tumors like SCCOHTs are immunogenic and exhibit biologically significant levels of T-cell infiltration and PD-L1 expression [40]. It has been reported that several patients with mutations in the SWI/SNF complex have benefited from checkpoint blockade immunotherapy [37, 39, 40]. Although immune checkpoint inhibitor treatment has shown promising results, only a minority of treated patients exhibit durable responses [40, 66]. Additionally, many of those who initially responded to treatment eventually experience relapse due to acquired drug resistance. As with conventional cancer therapies, one way to improve clinical responses with immune checkpoint blockade is through combination therapy strategies.

Numerous studies have revealed that epigenetic modulation plays a key role in tumor immune escape. Cancer cells show frequent loss or epigenetic silencing of the cytosolic DNA sensor cGAS and/or STING to promote immune evasion [67]. Conversely, aberrant LSD1 activity suppresses the expression of immune protective factors [61] such as PD-L1 and CTLA-4. Recently, it has been shown that inhibition of LSD1 significantly increases tumor immunogenicity [51] primarily through changes in methylation levels. To that end, increased levels of methylation promotes ERV expression, leading to dsRNA stress. Methylation of AGO2 results in destabilization of the integrity of the RISC complex and inhibition of dsRNA degradation. dsRNA stress activates IFN-dependent immune response that consequently sensitizes tumors to T-cell immunity and T-cell infiltration. As LSD1 is highly expressed in SCCOHT cell lines and interacts with members of the SWI/SNF complex to regulate gene expression [55, 68, 69], it is an ideal therapeutic target for the treatment of SCCOHT and potentially other SWI/SNF loss-of-function- dependent cancers.

In this study, we demonstrate that inhibition of LSD1 activity by the reversible inhibitor SP-2577 (Seclidemstat) induces the expression of ERVs and IFN β in SCCOHT. In agreement with the previous observation that LSD1 negatively regulates expression of chemokines and immune protective factors such as PD-L1 [61], inhibition of LSD1 with SP-2577 promoted expression of chemokines and PD-L1 in SCCOHT cell lines, which results in activation of T-cell infiltration.

The contribution of ERVs to the immune response is not limited to the dsRNA/MDA5 interaction followed by activation of the IFN pathway. Tumor neoantigen analysis has shown that ERVs can encode for strictly tumor-specific antigens, otherwise silent in normal tissue, capable of eliciting T cell-specific antitumor immunity. Schiavetti et al have shown that ERV-K antigens are highly expressed in a variety of malignancies such as breast, melanoma, sarcoma, lymphoma, and bladder cancer [70], and the ERV-E encoded antigen is selectively expressed in RCC kidney tumors [71]. Moreover, it has been shown that in epithelial OC and in colon cancer high levels of ERVs expression correlates robustly to immune checkpoint therapy response [72, 73]. Expression of ERV elements is subjected to genome-wide regulation by epigenetic silencing [74, 75]. However, many ERVs are still transcribed in adult cells and contribute to autoimmune pathologies such as systemic lupus erythematosus and Aicardi-Goutières syndrome [76]. Similarly, dysregulation of epigenetic pathways also contributes to reactivation of ERV elements in tumor cells [77].

SWI/SNF may play a role in the establishment of ERV silencing. In embryonic stem cells SMARCA4, a SWI/SNF-like chromatin remodeler, negatively regulates the retrotransposon activity through recruitment of KRAB associated protein 1 (KAP1) [78]. Docking KAP1 at the ERV elements in the genome triggers the formation of a complex with the histone methyltransferase SETDB1, resulting in formation of H3K9me3 and silencing of ERV class I and II.

Lack of SMARCA4 compromises the stability of KAP1-SETDB1 association at ERVs, which lead to reduction of H3K9me3 and activation of ERV transcription. Restoration of SMARCA4 activity reverses the ERV upregulation [78]. Similarly, SWI/SNF complex members, including SMARCA4 and LSH1, are known to ensure silencing of retrotransposons in the stem cells through interaction with DNMT3a and HDACs [75, 78]. Transcriptome analysis of RT cell lines with inducible SMARCB1 re-expression identified significant ERVs overexpression in SMARCB1-deficient conditions [79]. In support of this, our studies show that re-expression of SMARCA4 in SCCOHT or ARID1A in OCCC results in the loss of ERV expression and reduction of T-cell infiltration, even in the presence of conditioned medium enriched in cytokines and chemokines, implying that T-cell infiltration may be related to the loss of SWI/SNF complex function.

Together, these results suggest that SWI/SNF deficiency plays a crucial role on ERVs epigenetic silencing, resulting in enhancement of tumor immunogenicity. Moreover, LSD1-dependent histone modifications result in significant downregulation of ERVs [74, 80]. By inhibiting LSD1, SP-2577 ensures increased ERV activation and cytokine production, resulting in enhanced T cell immune response. In addition, SP-2577 treatment promotes PD-L1 expression, and co-treatment with α -PD-L1 or α -CTLA-4 antibodies significantly amplifies the CD8⁺ T-cell infiltration in SCCOHT and OCCC immune organoids.

Collectively, these findings demonstrate the important role of SP-2577 in the regulation of T-cell recruitment to the tumor microenvironment and highlight the potential of combining SP-2577 with checkpoint immunotherapy in SCCOHT, OCCC, and other SWI/SNF-mutated malignancies.

Supporting information

S1 Raw images. Original western blot and revert for Fig 6A. Western blot analysis for SMARCA4 expression level in COV 434 pIND20 BRG1-2.7 after 1 μ M doxycycline daily treatment for 5 days (D = days). Total protein load was verified by LSD1 expression analysis. A) SMARCA4; B) LSD1.

(PDF)

S1 Table. The cancer type acronym to full cancer type key from TCGA PanCancer Atlas.

(PDF)

S2 Table. List of primers used in qPCR.

(PDF)

Author Contributions

Conceptualization: Raffaella Soldi, Rhonda Lewis, Mohan R. Kaadige, Jeffrey M. Trent, William P. D. Hendricks, Sunil Sharma.

Data curation: Raffaella Soldi, Tithi Ghosh Halder, Alexis Weston, Hariprasad Vankayalapati.

Formal analysis: Raffaella Soldi.

Investigation: Raffaella Soldi, Tithi Ghosh Halder, Alexis Weston, Kevin Drenner.

Methodology: Raffaella Soldi, Tithi Ghosh Halder, Alexis Weston, Ryan Rodriguez del Villar.

Project administration: Sunil Sharma.

Software: Raffaella Soldi, Tithi Ghosh Halder, Alexis Weston, Kevin Drenner.

Supervision: Raffaella Soldi, Sunil Sharma.

Validation: Raffaella Soldi, Tithi Ghosh Halder.

Writing – original draft: Raffaella Soldi.

Writing – review & editing: Tithi Ghosh Halder, Trason Thode, Kevin Drenner, Rhonda Lewis, Mohan R. Kaadige, Shreyesi Srivastava, Sherin Daniel Ampanattu, Ryan Rodriguez del Villar, Jessica Lang, Bernard Weissman, William P. D. Hendricks, Sunil Sharma.

References

1. St Pierre R, Kadoch C. Mammalian SWI/SNF complexes in cancer: emerging therapeutic opportunities. *Curr Opin Genet Dev*. 2017; 42:56–67. <https://doi.org/10.1016/j.gde.2017.02.004> PMID: 28391084
2. Williams GM, Hume DM, Hudson RP Jr., Morris PJ, Kano K, Milgrom F. "Hyperacute" renal-homograft rejection in man. *N Engl J Med*. 1968; 279(12):611–8. <https://doi.org/10.1056/NEJM196809192791201> PMID: 4174539
3. Brownlee PM, Meisenberg C, Downs JA. The SWI/SNF chromatin remodelling complex: Its role in maintaining genome stability and preventing tumorigenesis. *DNA Repair (Amst)*. 2015; 32:127–33. <https://doi.org/10.1016/j.dnarep.2015.04.023> PMID: 25981841
4. Dutta A, Sardu M, Gogol M, Gilmore J, Zhang D, Florens L, et al. Composition and Function of Mutant Swi/Snf Complexes. *Cell Rep*. 2017; 18(9):2124–34. <https://doi.org/10.1016/j.celrep.2017.01.058> PMID: 28249159
5. Lu B, Shi H. An In-Depth Look at Small Cell Carcinoma of the Ovary, Hypercalcemic Type (SCCOHT): Clinical Implications from Recent Molecular Findings. *J Cancer*. 2019; 10(1):223–37. <https://doi.org/10.7150/jca.26978> PMID: 30662543
6. Agaimy A, Daum O, Markl B, Lichtmanegger I, Michal M, Hartmann A. SWI/SNF Complex-deficient Undifferentiated/Rhabdoid Carcinomas of the Gastrointestinal Tract: A Series of 13 Cases Highlighting Mutually Exclusive Loss of SMARCA4 and SMARCA2 and Frequent Co-inactivation of SMARCB1 and SMARCA2. *Am J Surg Pathol*. 2016; 40(4):544–53. <https://doi.org/10.1097/PAS.0000000000000554> PMID: 26551623
7. Ramalingam P, Croce S, McCluggage WG. Loss of expression of SMARCA4 (BRG1), SMARCA2 (BRM) and SMARCB1 (INI1) in undifferentiated carcinoma of the endometrium is not uncommon and is not always associated with rhabdoid morphology. *Histopathology*. 2017; 70(3):359–66. <https://doi.org/10.1111/his.13091> PMID: 27656868
8. Matsushita M, Kuwamoto S. Cytologic Features of SMARCA4-Deficient Thoracic Sarcoma: A Case Report and Comparison with Other SWI/SNF Complex-Deficient Tumors. *Acta Cytol*. 2018; 62(5–6):456–62. <https://doi.org/10.1159/000493335> PMID: 30286456
9. Yoshida A, Kobayashi E, Kubo T, Kodaira M, Motoi T, Motoi N, et al. Clinicopathological and molecular characterization of SMARCA4-deficient thoracic sarcomas with comparison to potentially related entities. *Mod Pathol*. 2017; 30(6):797–809. <https://doi.org/10.1038/modpathol.2017.11> PMID: 28256572
10. Pawel BR. SMARCB1-deficient Tumors of Childhood: A Practical Guide. *Pediatr Dev Pathol*. 2018; 21(1):6–28. <https://doi.org/10.1177/1093526617749671> PMID: 29280680
11. Biegel JA, Busse TM, Weissman BE. SWI/SNF chromatin remodeling complexes and cancer. *Am J Med Genet C Semin Med Genet*. 2014; 166C(3):350–66. <https://doi.org/10.1002/ajmg.c.31410> PMID: 25169151
12. Masliah-Planchon J, Bieche I, Guinebretiere JM, Bourdeaut F, Delattre O. SWI/SNF chromatin remodeling and human malignancies. *Annu Rev Pathol*. 2015; 10:145–71. <https://doi.org/10.1146/annurev-pathol-012414-040445> PMID: 25387058
13. Torre LA, Trabert B, DeSantis CE, Miller KD, Samimi G, Runowicz CD, et al. Ovarian cancer statistics, 2018. *CA Cancer J Clin*. 2018; 68(4):284–96. <https://doi.org/10.3322/caac.21456> PMID: 29809280
14. Kadoch C, Hargreaves DC, Hodges C, Elias L, Ho L, Ranish J, et al. Proteomic and bioinformatic analysis of mammalian SWI/SNF complexes identifies extensive roles in human malignancy. *Nat Genet*. 2013; 45(6):592–601. <https://doi.org/10.1038/ng.2628> PMID: 23644491
15. Fukumoto T, Magno E, Zhang R. SWI/SNF Complexes in Ovarian Cancer: Mechanistic Insights and Therapeutic Implications. *Mol Cancer Res*. 2018; 16(12):1819–25. <https://doi.org/10.1158/1541-7786.MCR-18-0368> PMID: 30037854
16. Jelinic P, Mueller JJ, Olvera N, Dao F, Scott SN, Shah R, et al. Recurrent SMARCA4 mutations in small cell carcinoma of the ovary. *Nat Genet*. 2014; 46(5):424–6. <https://doi.org/10.1038/ng.2922> PMID: 24658004

17. Karnezis AN, Wang Y, Ramos P, Hendricks WP, Oliva E, D'Angelo E, et al. Dual loss of the SWI/SNF complex ATPases SMARCA4/BRG1 and SMARCA2/BRM is highly sensitive and specific for small cell carcinoma of the ovary, hypercalcaemic type. *J Pathol.* 2016; 238(3):389–400. <https://doi.org/10.1002/path.4633> PMID: 26356327
18. Patibandla JR, Fehniger JE, Levine DA, Jelinic P. Small cell cancers of the female genital tract: Molecular and clinical aspects. *Gynecol Oncol.* 2018; 149(2):420–7. <https://doi.org/10.1016/j.ygyno.2018.02.004> PMID: 29458976
19. Jones S, Wang TL, Shih Ie M, Mao TL, Nakayama K, Roden R, et al. Frequent mutations of chromatin remodeling gene ARID1A in ovarian clear cell carcinoma. *Science.* 2010; 330(6001):228–31. <https://doi.org/10.1126/science.1196333> PMID: 20826764
20. Mabuchi S, Sugiyama T, Kimura T. Clear cell carcinoma of the ovary: molecular insights and future therapeutic perspectives. *J Gynecol Oncol.* 2016; 27(3):e31. <https://doi.org/10.3802/jgo.2016.27.e31> PMID: 27029752
21. del Carmen MG, Birrer M, Schorge JO. Clear cell carcinoma of the ovary: a review of the literature. *Gynecol Oncol.* 2012; 126(3):481–90. <https://doi.org/10.1016/j.ygyno.2012.04.021> PMID: 22525820
22. Qin Q, Ajewole VB, Sheu TG, Donohue R, Singh M. Successful treatment of a stage IIIC small-cell carcinoma of the ovary hypercalcaemic subtype using multi-modality therapeutic approach. *Ecancermedicallscience.* 2018; 12:832. <https://doi.org/10.3332/ecancer.2018.832> PMID: 29910829
23. Young RH, Oliva E, Scully RE. Small cell carcinoma of the ovary, hypercalcaemic type. A clinicopathological analysis of 150 cases. *Am J Surg Pathol.* 1994; 18(11):1102–16. <https://doi.org/10.1097/0000478-199411000-00004> PMID: 7943531
24. Mayes K, Qiu Z, Alhazmi A, Landry JW. ATP-dependent chromatin remodeling complexes as novel targets for cancer therapy. *Adv Cancer Res.* 2014; 121:183–233. <https://doi.org/10.1016/B978-0-12-800249-0.00005-6> PMID: 24889532
25. Hoffman GR, Rahal R, Buxton F, Xiang K, McAllister G, Frias E, et al. Functional epigenetics approach identifies BRM/SMARCA2 as a critical synthetic lethal target in BRG1-deficient cancers. *Proc Natl Acad Sci U S A.* 2014; 111(8):3128–33. <https://doi.org/10.1073/pnas.1316793111> PMID: 24520176
26. Oike T, Ogiwara H, Tominaga Y, Ito K, Ando O, Tsuta K, et al. A synthetic lethality-based strategy to treat cancers harboring a genetic deficiency in the chromatin remodeling factor BRG1. *Cancer Res.* 2013; 73(17):5508–18. <https://doi.org/10.1158/0008-5472.CAN-12-4593> PMID: 23872584
27. Romero OA, Torres-Diz M, Pros E, Savola S, Gomez A, Moran S, et al. MAX inactivation in small cell lung cancer disrupts MYC-SWI/SNF programs and is synthetic lethal with BRG1. *Cancer Discov.* 2014; 4(3):292–303. <https://doi.org/10.1158/2159-8290.CD-13-0799> PMID: 24362264
28. Caumanns JJ, Wisman GBA, Berns K, van der Zee AGJ, de Jong S. ARID1A mutant ovarian clear cell carcinoma: A clear target for synthetic lethal strategies. *Biochim Biophys Acta Rev Cancer.* 2018; 1870(2):176–84. <https://doi.org/10.1016/j.bbcan.2018.07.005> PMID: 30025943
29. Lang JD, Hendricks WPD, Orlando KA, Yin H, Kiefer J, Ramos P, et al. Ponatinib Shows Potent Antitumor Activity in Small Cell Carcinoma of the Ovary Hypercalcaemic Type (SCCOHT) through Multikinase Inhibition. *Clin Cancer Res.* 2018; 24(8):1932–43. <https://doi.org/10.1158/1078-0432.CCR-17-1928> PMID: 29440177
30. Chan-Penebre E, Armstrong K, Drew A, Grassian AR, Feldman I, Knutson SK, et al. Selective Killing of SMARCA2- and SMARCA4-deficient Small Cell Carcinoma of the Ovary, Hypercalcaemic Type Cells by Inhibition of EZH2: In Vitro and In Vivo Preclinical Models. *Mol Cancer Ther.* 2017; 16(5):850–60. <https://doi.org/10.1158/1535-7163.MCT-16-0678> PMID: 28292935
31. Kim KH, Kim W, Howard TP, Vazquez F, Tsherniak A, Wu JN, et al. SWI/SNF-mutant cancers depend on catalytic and non-catalytic activity of EZH2. *Nat Med.* 2015; 21(12):1491–6. <https://doi.org/10.1038/nm.3968> PMID: 26552009
32. Wang Y, Chen SY, Karnezis AN, Colborne S, Santos ND, Lang JD, et al. The histone methyltransferase EZH2 is a therapeutic target in small cell carcinoma of the ovary, hypercalcaemic type. *J Pathol.* 2017; 242(3):371–83. <https://doi.org/10.1002/path.4912> PMID: 28444909
33. Wang Y, Chen SY, Colborne S, Lambert G, Shin CY, Santos ND, et al. Histone Deacetylase Inhibitors Synergize with Catalytic Inhibitors of EZH2 to Exhibit Antitumor Activity in Small Cell Carcinoma of the Ovary, Hypercalcaemic Type. *Mol Cancer Ther.* 2018; 17(12):2767–79. <https://doi.org/10.1158/1535-7163.MCT-18-0348> PMID: 30232145
34. Shorstova T, Marques M, Su J, Johnston J, Kleinman CL, Hamel N, et al. SWI/SNF-Compromised Cancers Are Susceptible to Bromodomain Inhibitors. *Cancer Res.* 2019; 79(10):2761–74. <https://doi.org/10.1158/0008-5472.CAN-18-1545> PMID: 30877105
35. Xue Y, Meehan B, Fu Z, Wang XQD, Fiset PO, Rieker R, et al. SMARCA4 loss is synthetic lethal with CDK4/6 inhibition in non-small cell lung cancer. *Nat Commun.* 2019; 10(1):557. <https://doi.org/10.1038/s41467-019-08380-1> PMID: 30718506

36. Xue Y, Meehan B, Macdonald E, Venneti S, Wang XQD, Witkowski L, et al. CDK4/6 inhibitors target SMARCA4-determined cyclin D1 deficiency in hypercalcemic small cell carcinoma of the ovary. *Nat Commun.* 2019; 10(1):558. <https://doi.org/10.1038/s41467-018-06958-9> PMID: 30718512
37. Miao D, Margolis CA, Gao W, Voss MH, Li W, Martini DJ, et al. Genomic correlates of response to immune checkpoint therapies in clear cell renal cell carcinoma. *Science.* 2018; 359(6377):801–6. <https://doi.org/10.1126/science.aan5951> PMID: 29301960
38. Motzer RJ, Tannir NM, McDermott DF, Aren Frontera O, Melichar B, Choueiri TK, et al. Nivolumab plus Ipilimumab versus Sunitinib in Advanced Renal-Cell Carcinoma. *N Engl J Med.* 2018; 378(14):1277–90. <https://doi.org/10.1056/NEJMoa1712126> PMID: 29562145
39. Pan D, Kobayashi A, Jiang P, Ferrari de Andrade L, Tay RE, Luoma AM, et al. A major chromatin regulator determines resistance of tumor cells to T cell-mediated killing. *Science.* 2018; 359(6377):770–5. <https://doi.org/10.1126/science.aao1710> PMID: 29301958
40. Jelinic P, Ricca J, Van Oudenhove E, Olvera N, Merghoub T, Levine DA, et al. Immune-Active Microenvironment in Small Cell Carcinoma of the Ovary, Hypercalcemic Type: Rationale for Immune Checkpoint Blockade. *J Natl Cancer Inst.* 2018; 110(7):787–90. <https://doi.org/10.1093/jnci/djx277> PMID: 29365144
41. Fukumoto T, Fatkhutdinov N, Zundell JA, Tcyganov EN, Nacarelli T, Karakashev S, et al. HDAC6 Inhibition Synergizes with Anti-PD-L1 Therapy in ARID1A-Inactivated Ovarian Cancer. *Cancer Res.* 2019; 79(21):5482–9. <https://doi.org/10.1158/0008-5472.CAN-19-1302> PMID: 31311810
42. Hamanishi J, Mandai M, Ikeda T, Minami M, Kawaguchi A, Murayama T, et al. Safety and Antitumor Activity of Anti-PD-1 Antibody, Nivolumab, in Patients With Platinum-Resistant Ovarian Cancer. *J Clin Oncol.* 2015; 33(34):4015–22. <https://doi.org/10.1200/JCO.2015.62.3397> PMID: 26351349
43. Ambrosio S, Sacca CD, Amente S, Paladino S, Lania L, Majello B. Lysine-specific demethylase LSD1 regulates autophagy in neuroblastoma through SESN2-dependent pathway. *Oncogene.* 2017; 36(48):6701–11. <https://doi.org/10.1038/onc.2017.267> PMID: 28783174
44. Amente S, Lania L, Majello B. The histone LSD1 demethylase in stemness and cancer transcription programs. *Biochim Biophys Acta.* 2013; 1829(10):981–6. <https://doi.org/10.1016/j.bbagra.2013.05.002> PMID: 23684752
45. Schulte JH, Lim S, Schramm A, Friedrichs N, Koster J, Versteeg R, et al. Lysine-specific demethylase 1 is strongly expressed in poorly differentiated neuroblastoma: implications for therapy. *Cancer Res.* 2009; 69(5):2065–71. <https://doi.org/10.1158/0008-5472.CAN-08-1735> PMID: 19223552
46. Huang J, Sengupta R, Espejo AB, Lee MG, Dorsey JA, Richter M, et al. p53 is regulated by the lysine demethylase LSD1. *Nature.* 2007; 449(7158):105–8. <https://doi.org/10.1038/nature06092> PMID: 17805299
47. Kontaki H, Talianidis I. Cross-talk between post-translational modifications regulate life or death decisions by E2F1. *Cell Cycle.* 2010; 9(19):3836–7. <https://doi.org/10.4161/cc.9.19.13384> PMID: 20890118
48. Kontaki H, Talianidis I. Lysine methylation regulates E2F1-induced cell death. *Mol Cell.* 2010; 39(1):152–60. <https://doi.org/10.1016/j.molcel.2010.06.006> PMID: 20603083
49. Scoumanne A, Chen X. The lysine-specific demethylase 1 is required for cell proliferation in both p53-dependent and -independent manners. *J Biol Chem.* 2007; 282(21):15471–5. <https://doi.org/10.1074/jbc.M701023200> PMID: 17409384
50. Wang J, Hevi S, Kurash JK, Lei H, Gay F, Bajko J, et al. The lysine demethylase LSD1 (KDM1) is required for maintenance of global DNA methylation. *Nat Genet.* 2009; 41(1):125–9. <https://doi.org/10.1038/ng.268> PMID: 19098913
51. Sheng W, LaFleur MW, Nguyen TH, Chen S, Chakravarthy A, Conway JR, et al. LSD1 Ablation Stimulates Anti-tumor Immunity and Enables Checkpoint Blockade. *Cell.* 2018; 174(3):549–63 e19. <https://doi.org/10.1016/j.cell.2018.05.052> PMID: 29937226
52. Chen S, Lee LF, Fisher TS, Jessen B, Elliott M, Evering W, et al. Combination of 4-1BB agonist and PD-1 antagonist promotes antitumor effector/memory CD8 T cells in a poorly immunogenic tumor model. *Cancer Immunol Res.* 2015; 3(2):149–60. <https://doi.org/10.1158/2326-6066.CIR-14-0118> PMID: 25387892
53. Juneja VR, McGuire KA, Manguso RT, LaFleur MW, Collins N, Haining WN, et al. PD-L1 on tumor cells is sufficient for immune evasion in immunogenic tumors and inhibits CD8 T cell cytotoxicity. *J Exp Med.* 2017; 214(4):895–904. <https://doi.org/10.1084/jem.20160801> PMID: 28302645
54. Hiramatsu H, Kobayashi K, Kobayashi K, Haraguchi T, Ino Y, Todo T, et al. The role of the SWI/SNF chromatin remodeling complex in maintaining the stemness of glioma initiating cells. *Sci Rep.* 2017; 7(1):889. <https://doi.org/10.1038/s41598-017-00982-3> PMID: 28420882
55. Rossbach M. Non-Coding RNAs in Neural Networks, REST-Assured. *Front Genet.* 2011; 2:8. <https://doi.org/10.3389/fgene.2011.00008> PMID: 22303307

56. Nacht AS, Pohl A, Zaurin R, Soronellas D, Quilez J, Sharma P, et al. Hormone-induced repression of genes requires BRG1-mediated H1.2 deposition at target promoters. *EMBO J*. 2016; 35(16):1822–43. <https://doi.org/10.15252/embj.201593260> PMID: 27390128
57. Yatim A, Benne C, Sobhian B, Laurent-Chabalier S, Deas O, Judde JG, et al. NOTCH1 nuclear interactome reveals key regulators of its transcriptional activity and oncogenic function. *Mol Cell*. 2012; 48(3):445–58. <https://doi.org/10.1016/j.molcel.2012.08.022> PMID: 23022380
58. Sorna V, Theisen ER, Stephens B, Warner SL, Bearss DJ, Vankayalapati H, et al. High-throughput virtual screening identifies novel N¹-(1-phenylethylidene)-benzohydrazides as potent, specific, and reversible LSD1 inhibitors. *J Med Chem*. 2013; 56(23):9496–508. <https://doi.org/10.1021/jm400870h> PMID: 24237195
59. Cerami E, Gao J, Dogrusoz U, Gross BE, Sumer SO, Aksoy BA, et al. The cBio cancer genomics portal: an open platform for exploring multidimensional cancer genomics data. *Cancer Discov*. 2012; 2(5):401–4. <https://doi.org/10.1158/2159-8290.CD-12-0095> PMID: 22588877
60. Gao J, Aksoy BA, Dogrusoz U, Dresdner G, Gross B, Sumer SO, et al. Integrative analysis of complex cancer genomics and clinical profiles using the cBioPortal. *Sci Signal*. 2013; 6(269):pl1. <https://doi.org/10.1126/scisignal.2004088> PMID: 23550210
61. Qin Y, Vasilatos SN, Chen L, Wu H, Cao Z, Fu Y, et al. Inhibition of histone lysine-specific demethylase 1 elicits breast tumor immunity and enhances antitumor efficacy of immune checkpoint blockade. *Oncogene*. 2019; 38(3):390–405. <https://doi.org/10.1038/s41388-018-0451-5> PMID: 30111819
62. Bally AP, Austin JW, Boss JM. Genetic and Epigenetic Regulation of PD-1 Expression. *J Immunol*. 2016; 196(6):2431–7. <https://doi.org/10.4049/jimmunol.1502643> PMID: 26945088
63. Chi T. A BAF-centred view of the immune system. *Nat Rev Immunol*. 2004; 4(12):965–77. <https://doi.org/10.1038/nri1501> PMID: 15573131
64. Ni Z, Karaskov E, Yu T, Callaghan SM, Der S, Park DS, et al. Apical role for BRG1 in cytokine-induced promoter assembly. *Proc Natl Acad Sci U S A*. 2005; 102(41):14611–6. <https://doi.org/10.1073/pnas.0503070102> PMID: 16195385
65. Shen J, Ju Z, Zhao W, Wang L, Peng Y, Ge Z, et al. ARID1A deficiency promotes mutability and potentiates therapeutic antitumor immunity unleashed by immune checkpoint blockade. *Nat Med*. 2018; 24(5):556–62. <https://doi.org/10.1038/s41591-018-0012-z> PMID: 29736026
66. Naito T, Umemura S, Nakamura H, Zenke Y, Udagawa H, Kirita K, et al. Successful treatment with nivolumab for SMARCA4-deficient non-small cell lung carcinoma with a high tumor mutation burden: A case report. *Thorac Cancer*. 2019; 10(5):1285–8. <https://doi.org/10.1111/1759-7714.13070> PMID: 30972962
67. Xia T, Konno H, Ahn J, Barber GN. Deregulation of STING Signaling in Colorectal Carcinoma Constrains DNA Damage Responses and Correlates With Tumorigenesis. *Cell Rep*. 2016; 14(2):282–97. <https://doi.org/10.1016/j.celrep.2015.12.029> PMID: 26748708
68. Curtis BJ, Zraly CB, Marendra DR, Dingwall AK. Histone lysine demethylases function as co-repressors of SWI/SNF remodeling activities during *Drosophila* wing development. *Dev Biol*. 2011; 350(2):534–47. <https://doi.org/10.1016/j.ydbio.2010.12.001> PMID: 21146519
69. Hiramatsu H, Kobayashi K, Kobayashi K, Haraguchi T, Ino Y, Todo T, et al. Author Correction: The role of the SWI/SNF chromatin remodeling complex in maintaining the stemness of glioma initiating cells. *Sci Rep*. 2018; 8(1):16079. <https://doi.org/10.1038/s41598-018-31444-z> PMID: 30356171
70. Schiavetti F, Thonnard J, Colau D, Boon T, Coulie PG. A human endogenous retroviral sequence encoding an antigen recognized on melanoma by cytolytic T lymphocytes. *Cancer Res*. 2002; 62(19):5510–6. PMID: 12359761
71. Improgo MR, Soll LG, Tapper AR, Gardner PD. Nicotinic acetylcholine receptors mediate lung cancer growth. *Front Physiol*. 2013; 4:251. <https://doi.org/10.3389/fphys.2013.00251> PMID: 24062692
72. Chiappinelli KB, Strissel PL, Desrichard A, Li H, Henke C, Akman B, et al. Inhibiting DNA Methylation Causes an Interferon Response in Cancer via dsRNA Including Endogenous Retroviruses. *Cell*. 2015; 162(5):974–86. <https://doi.org/10.1016/j.cell.2015.07.011> PMID: 26317466
73. Le DT, Uram JN, Wang H, Bartlett BR, Kemberling H, Eyring AD, et al. PD-1 Blockade in Tumors with Mismatch-Repair Deficiency. *N Engl J Med*. 2015; 372(26):2509–20. <https://doi.org/10.1056/NEJMoa1500596> PMID: 26028255
74. Leung DC, Lorincz MC. Silencing of endogenous retroviruses: when and why do histone marks predominate? *Trends Biochem Sci*. 2012; 37(4):127–33. <https://doi.org/10.1016/j.tibs.2011.11.006> PMID: 22178137
75. Maksakova IA, Mager DL, Reiss D. Keeping active endogenous retroviral-like elements in check: the epigenetic perspective. *Cell Mol Life Sci*. 2008; 65(21):3329–47. <https://doi.org/10.1007/s00018-008-8494-3> PMID: 18818875

76. Kassiotis G, Stoye JP. Immune responses to endogenous retroelements: taking the bad with the good. *Nat Rev Immunol*. 2016; 16(4):207–19. <https://doi.org/10.1038/nri.2016.27> PMID: 27026073
77. Szpakowski S, Sun X, Lage JM, Dyer A, Rubinstein J, Kowalski D, et al. Loss of epigenetic silencing in tumors preferentially affects primate-specific retroelements. *Gene*. 2009; 448(2):151–67. <https://doi.org/10.1016/j.gene.2009.08.006> PMID: 19699787
78. Sachs P, Ding D, Bergmaier P, Lamp B, Schlagheck C, Finkernagel F, et al. SMARCAD1 ATPase activity is required to silence endogenous retroviruses in embryonic stem cells. *Nat Commun*. 2019; 10(1):1335. <https://doi.org/10.1038/s41467-019-09078-0> PMID: 30902974
79. Leruste A, Tosello J, Ramos RN, Tauziède-Espariat A, Brohard S, Han ZY, et al. Clonally Expanded T Cells Reveal Immunogenicity of Rhabdoid Tumors. *Cancer Cell*. 2019; 36(6):597–612 e8. <https://doi.org/10.1016/j.ccell.2019.10.008> PMID: 31708437
80. Macfarlan TS, Gifford WD, Agarwal S, Driscoll S, Lettieri K, Wang J, et al. Endogenous retroviruses and neighboring genes are coordinately repressed by LSD1/KDM1A. *Genes Dev*. 2011; 25(6):594–607. <https://doi.org/10.1101/gad.2008511> PMID: 21357675